Bond and site percolation in three dimensions

Junfeng Wang, Zongzheng Zhou, Wei Zhang, Timothy M. Garoni, and Youjin Deng

Phys. Rev. E **87**, 052107 — Published 7 May 2013

DOI: 10.1103/PhysRevE.87.052107

Bond and Site Percolation in Three Dimensions

Junfeng Wang,[1] Zongzheng Zhou,[1,2] Wei Zhang,[3] Timothy M. Garoni,[2,*] and Youjin Deng[1,†]

[1]*Hefei National Laboratory for Physical Sciences at Microscale and Department of Modern Physics, University of Science and Technology of China, Hefei, Anhui 230026, China*
[2]*School of Mathematical Sciences, Monash University, Clayton, Victoria 3800, Australia*
[3]*Department of Physics, Jinan University, Guangzhou 510632, China*

We simulate the bond and site percolation models on the simple-cubic lattice with linear sizes up to $L = 512$, and estimate the percolation thresholds to be $p_c(\text{bond}) = 0.248\,811\,82(10)$ and $p_c(\text{site}) = 0.311\,607\,7(2)$. By performing extensive simulations at these estimated critical points, we then estimate the critical exponents $1/\nu = 1.141\,0(15)$, $\beta/\nu = 0.477\,05(15)$, the leading correction exponent $y_i = -1.2(2)$, and the shortest-path exponent $d_{\min} = 1.375\,6(3)$. Various universal amplitudes are also obtained, including wrapping probabilities, ratios associated with the cluster-size distribution, and the excess cluster number. We observe that the leading finite-size corrections in certain wrapping probabilities are governed by an exponent ≈ -2, rather than $y_i \approx -1.2$.

PACS numbers: 05.50.+q (lattice theory and statistics), 05.70.Jk (critical point phenomena), 64.60.ah (percolation), 64.60.F- (equilibrium properties near critical points, critical exponents)
Keywords:

I. INTRODUCTION

Percolation [1] is a cornerstone of the theory of critical phenomena [2], and a central topic in probability [3, 4]. In two dimensions, Coulomb gas arguments [5] and conformal field theory [6] predict the exact values of the bulk critical exponents $\beta = 5/36$, $\nu = 4/3$, which have been confirmed rigorously in the specific case of triangular-lattice site percolation [7]. Exact values of the percolation thresholds p_c on several two-dimensional lattices are also known [8]. In particular, it is known rigorously [9] that $p_c = 1/2$ for bond percolation on the square lattice. For all d greater than or equal to the upper critical dimension [10] of $d_c = 6$, the mean-field values for the exponents $\beta = 1$, $d\nu = 3$ are believed to hold; this has been proved rigorously [11, 12] for $d \geq 19$.

For dimensions $2 < d < 6$ by contrast, no exact values for either the critical exponents or percolation thresholds are known. Significant effort has therefore been expended on obtaining ever more accurate estimates, especially in three dimensions.

In addition to percolation thresholds and critical exponents, crossing probabilities [13, 14] also play an important role in studies of percolation. For lattices drawn on a torus, the analogous quantities are wrapping probabilities [15], and in two dimensions their values can be determined exactly [16]. The three-dimensional case [17] has been far less studied however. Precisely estimating wrapping probabilities on the simple-cubic lattice represents one of the central undertakings of the current work.

In addition to their intrinsic importance, wrapping probabilities have proved to be an effective practical means of estimating percolation thresholds [18, 19]. Using Monte Carlo (MC) simulations and performing a careful finite-size scaling analysis of various wrapping probabilities in the neighbourhood of the transition, we obtain very accurate estimates of p_c for both site and bond percolation. We observe numerically that the leading finite-size corrections for certain wrapping probabilities appear to be governed by an exponent ≈ -2, rather than by the leading irrelevant exponent $y_i \approx -1.2$.

We then estimate the thermal exponent $y_t = 1/\nu$ by fixing p to our best estimate of p_c, and studying the divergence with linear size L of the derivative of the wrapping probability, which is proportional to the covariance of its indicator with the number of bonds. We find this procedure for estimating y_t preferable to methods in which y_t is estimated by studying how quantities behave in a neighbourhood of p values around p_c. In particular, we believe the current method produces more reliable error estimates.

The remainder of this paper is organized as follows. The simulation method and the sampled quantities are discussed in Section II. The results for the wrapping probabilities and thresholds are given in Section III. Critical exponents and the excess cluster number are discussed in Section IV. We then finally conclude with a discussion in Section V.

II. SAMPLED QUANTITIES

We study bond and site percolation on the periodic $L \times L \times L$ simple-cubic lattice with linear system sizes $L = 8$, 12, 16, 24, 32, 48, 64, 128, 256, 512. For each system size, we produced at least 2.5×10^7 independent samples. Each independent bond (site) configuration is generated by independently occupying each bond (site) with probability p. The clusters in each configuration are identified using breadth-first search. The number of sites in each cluster defines its size.

*Electronic address: tim.garoni@monash.edu
†Electronic address: yjdeng@ustc.edu.cn

TABLE I: Fits of the wrapping probabilities $R^{(x)}, R^{(a)}, R^{(3)}$, and the ratios Q_1, Q_2 for bond percolation. We did not obtain stable fits with y_i free for $R^{(3)}$.

	$L_{\min}$	χ^2/DF	p_c	y_t	$\mathcal{O}_c$	q_1	b_1	y_i	b_2
Q_1	16	53/40	0.248 812 03(5)	1.16(1)	0.865 37(1)	−0.36(1)	−0.0423(5)	−1.2	0.341(5)
	24	33/33	0.248 811 98(6)	1.16(2)	0.865 35(2)	−0.31(2)	−0.040(2)	−1.2	0.31(2)
	32	28/26	0.248 811 93(7)	1.19(3)	0.865 33(2)	−0.31(3)	−0.036(3)	−1.2	0.25(5)
	16	44/39	0.248 811 84(8)	1.16(1)	0.865 39(3)	−0.36(1)	−0.10(4)	−1.34(9)	0.50(8)
	24	31/32	0.248 811 88(9)	1.19(2)	0.865 29(4)	−0.32(3)	−0.10(8)	−1.3(2)	0.5(2)
	32	28/25	0.248 811 96(14)	1.19(3)	0.865 4(2)	−0.31(3)	−0.02(4)	−1.0(5)	0.2(3)
Q_2	32	28/25	0.248 811 20(5)	1.17(2)	0.633 58(3)	−0.80(5)	−0.104(4)	−1.2	0.05(7)
	48	16/18	0.248 811 95(6)	1.14(2)	0.633 50(3)	−0.89(8)	−0.088(9)	−1.2	−0.3(2)
	64	10/11	0.248 811 84(11)	1.12(3)	0.633 4(2)	−1.0(2)	−0.05(4)	−1.2	−1(1)
	32	28/26	0.248 812 02(6)	1.17(2)	0.633 58(5)	−0.80(5)	−0.097(8)	−1.08(3)	-
	48	16/19	0.248 811 93(7)	1.14(2)	0.633 46(7)	−0.89(8)	−0.15(4)	−1.22(7)	-
	64	10/12	0.248 811 82(11)	1.12(3)	0.633 3(2)	−1.0(2)	−0.5(6)	−1.5(4)	-
$R^{(x)}$	16	41/37	0.248 811 81(4)	1.143(7)	0.257 77(2)	−1.22(3)	0.005(2)	−1.2	−0.23(1)
	24	30/31	0.248 811 83(4)	1.15(2)	0.257 78(3)	−1.22(6)	0.003(3)	−1.2	−0.26(4)
	32	25/24	0.248 811 82(6)	1.15(2)	0.257 76(5)	−1.20(8)	0.006(7)	−1.2	−0.20(10)
	16	41/37	0.248 811 82(4)	1.144(7)	0.257 79(2)	−1.22(3)	0.18(2)	−1.83(4)	-
	24	31/31	0.248 811 84(4)	1.15(2)	0.257 79(2)	−1.22(6)	0.22(8)	−1.9(2)	-
	32	25/24	0.248 811 82(6)	1.15(2)	0.257 77(4)	−1.20(8)	0.1(1)	−1.7(3)	-
$R^{(a)}$	16	40/39	0.248 811 82(4)	1.149(7)	0.459 99(3)	−1.65(4)	0.004(2)	−1.2	0.73(2)
	24	25/32	0.248 811 82(5)	1.14(2)	0.459 97(5)	−1.74(9)	0.003(4)	−1.2	0.72(6)
	32	22/25	0.248 811 83(6)	1.14(2)	0.459 98(7)	−1.7(2)	0.005(9)	−1.2	0.7(2)
	16	40/39	0.248 811 82(4)	1.149(7)	0.459 97(2)	−1.65(4)	0.81(6)	−2.06(3)	-
	24	25/32	0.248 811 82(4)	1.14(2)	0.459 95(3)	−1.74(9)	0.8(2)	−2.05(8)	-
	32	22/25	0.248 811 82(5)	1.14(2)	0.459 96(5)	−1.74(2)	1.0(9)	−2.1(3)	-
$R^{(3)}$	16	44/38	0.248 811 85(6)	1.14(1)	0.080 41(2)	−0.66(2)	0.010(1)	−1.2	−0.076(8)
	24	35/31	0.248 811 91(6)	1.15(2)	0.080 43(3)	−0.63(5)	0.007(3)	−1.2	−0.04(3)
	32	23/24	0.248 811 85(8)	1.17(3)	0.080 39(4)	−0.59(5)	0.014(6)	−1.2	−0.15(9)

We sampled the following observables in our simulations:

- The number of occupied bonds $\mathcal{N}_b$ for bond percolation, and the number of occupied sites $\mathcal{N}_s$ for site percolation;
- The number of clusters $\mathcal{N}_c$;
- The size $\mathcal{C}_1$ of the largest cluster;
- The cluster-size moments $\mathcal{S}_m = \sum_C |C|^m$ with $m = 0, 2, 4$. The sum runs over all clusters C, and $\mathcal{S}_0$ is simply the number of clusters;
- An observable $\mathcal{S} := \max_C \max_{y \in C} d(x_C, y)$ used to determine the shortest-path exponent. Here $d(x, y)$ denotes the graph distance from site x to site y, and x_C is the vertex in cluster C with the smallest vertex label, according to some fixed (but arbitrary) vertex labeling.
- The indicators $\mathcal{R}^{(x)}$, $\mathcal{R}^{(y)}$, and $\mathcal{R}^{(z)}$, for the event that a cluster wraps around the lattice in the x, y, or z directions, respectively.

From these observables we calculated the following quantities:

- The mean size of the largest cluster $C_1 = \langle \mathcal{C}_1 \rangle$, which at p_c scales like $C_1 \sim L^{y_h}$ with $y_h = d_f = d - \beta/\nu$, where d_f is the fractal dimension;
- The cluster density $\rho = \langle \mathcal{N}_c \rangle / L^d$;
- The mean size of the cluster at the origin, $\chi = \langle \mathcal{S}_2 \rangle / L^d$, which at p_c scales like $\chi \sim L^{2y_h - d}$;
- The dimensionless ratios

$$Q_1 = \frac{\langle {\mathcal{C}_1}^2 \rangle}{\langle \mathcal{C}_1 \rangle^2} , \quad Q_2 = \frac{\langle {\mathcal{S}_2}^2 \rangle}{\langle 3{\mathcal{S}_2}^2 - 2\mathcal{S}_4 \rangle} ; \tag{1}$$

- The shortest-path length $S = \langle \mathcal{S} \rangle$, which at p_c scales like $S \sim L^{d_{\min}}$ with $d_{\min}$ the shortest-path fractal dimension;
- The wrapping probabilities

$$\begin{aligned} R^{(x)} &= \langle \mathcal{R}^{(x)} \rangle = \langle \mathcal{R}^{(y)} \rangle = \langle \mathcal{R}^{(z)} \rangle , \\ R^{(a)} &= 1 - \langle (1 - \mathcal{R}^{(x)})(1 - \mathcal{R}^{(y)})(1 - \mathcal{R}^{(z)}) \rangle , \\ R^{(3)} &= \langle \mathcal{R}^{(x)} \mathcal{R}^{(y)} \mathcal{R}^{(z)} \rangle . \end{aligned} \tag{2}$$

Here $R^{(x)}$ gives the probability that a winding exists in the x direction, $R^{(a)}$ gives the probability that a winding exists in at least one of

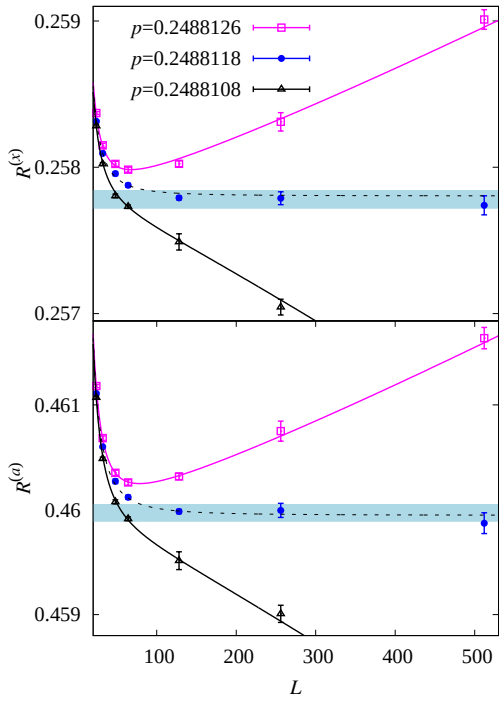

FIG. 1: Plots of $R^{(x)}(p,L)$ (top) and $R^{(a)}(p,L)$ (bottom) vs L for fixed values of p, for bond percolation. In both cases, the curves correspond to our preferred fit of the MC data for $R(p,L)$ by the ansatz (4); the dashed curve corresponds to setting $p = 0.248\,811\,82$. The blue strips indicate an interval of one sigma above and below the estimates $R_c^{(x)} = 0.257\,78(6)$ and $R_c^{(a)} = 0.459\,97(8)$.

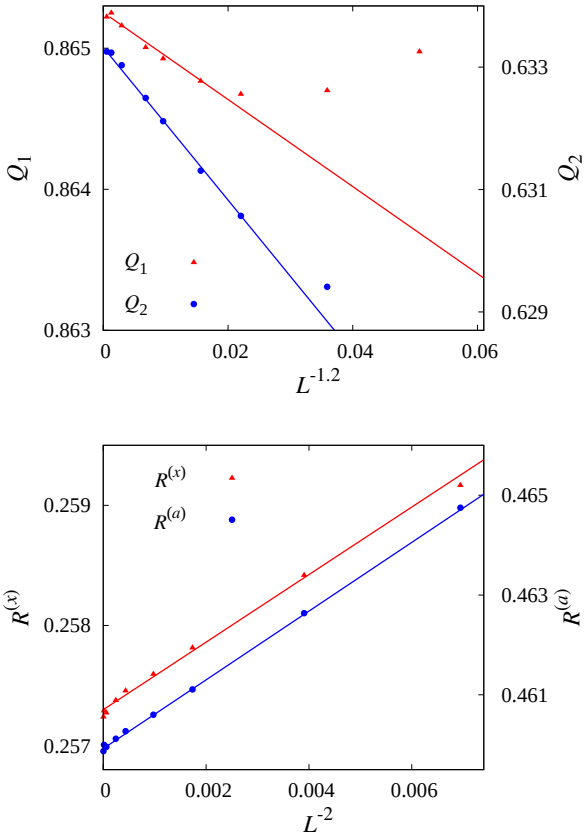

FIG. 2: Plots of Q_1 and Q_2 vs $L^{-1.2}$ (top), and $R^{(x)}$ and $R^{(a)}$ vs L^{-2} (bottom), with $p = 0.248\,811\,8$, for bond percolation. The solid lines are simply to guide the eye.

the three possible directions, and $R^{(3)}$ gives the probability that windings simultaneously exist in all three possible directions. Near p_c, we expect each of these wrapping probabilities to behave as $\sim f((p-p_c)L^{y_t})$, where f is a scaling function;

- The covariance of $\mathcal{R}^{(x)}$ and $\mathcal{N}_b$

$$g_{bR}^{(x)} = \langle \mathcal{R}^{(x)} \mathcal{N}_b \rangle - \langle \mathcal{R}^{(x)} \rangle \langle \mathcal{N}_b \rangle = p(1-p) \frac{\partial R^{(x)}}{\partial p} \,. \tag{3}$$

At p_c, we expect $g_{bR}^{(x)} \sim L^{y_t}$. An analogous definition of $g_{sR}^{(x)}$, with $\mathcal{N}_b$ being replaced with $\mathcal{N}_s$, was used for site percolation.

To derive (3), one can explicitly differentiate $\langle \mathcal{R}^{(x)} \rangle$ with respect to p, and use the fact that $\langle \mathcal{N}_b \rangle = p|E|$ where $|E|$ is the total number of edges on the lattice.

The complete set of data for all observables, for both bond and site percolation, is contained as a file `percolation.tar.gz` in the preprint version of this paper at arXiv.org [28].

III. ESTIMATING p_c

A. Bond percolation

We estimate the thresholds of bond and site percolation by studying the finite-size scaling of the wrapping probabilities $R^{(x)}$, $R^{(a)}$, $R^{(3)}$, and the dimensionless ratios Q_1, Q_2. Around p_c, we perform least-squares fits of the MC data for these quantities by the ansatz

$$\mathcal{O}(\epsilon, L) = \mathcal{O}_c + \sum_{k=1}^{2} q_k \epsilon^k L^{k y_t} + b_1 L^{y_i} + b_2 L^{-2} \quad , \tag{4}$$

where $\epsilon = p_c - p$, $\mathcal{O}_c$ is a universal constant, and y_i is the leading correction exponent. We perform fits with both b_1 and b_2 free, as well as fits with b_2 being set identically to zero. By performing fits with y_i free we estimate that $y_i = -1.2(2)$. We also perform fits with y_i fixed to $y_i = -1.2$.

As a precaution against correction-to-scaling terms that we have neglected in our chosen ansatz, we impose a lower cutoff $L \geq L_{\min}$ on the data points admitted in the fit, and we systematically study the effect on the χ^2 value of increasing $L_{\min}$. In general, our preferred fit for any

given ansatz corresponds to the smallest $L_{\min}$ for which χ^2 divided by the number of degrees of freedom (DF) is $O(1)$, and for which subsequent increases in $L_{\min}$ do not cause χ^2 to drop by vastly more than one unit per degree of freedom.

Table I summarizes the results of these fits. From the fits, we can see the finite-size corrections of Q_1 and Q_2 are dominated by the exponent $y_i \approx -1.2$. From Q_1 and Q_2, we estimate $p_c = 0.248\,811\,9(3)$, and their universal critical values $Q_{1,c} = 0.865\,4(2)$ and $Q_{2,c} = 0.633\,5(2)$.

For $R^{(x)}$ and $R^{(a)}$, fixing $y_i = -1.2$ and including both the b_1 and b_2 terms we find that b_1 is consistent with zero, while b_2 is clearly nonzero. Furthermore, if we set $b_2 = 0$ and leave y_i free, we find $y_i \approx -2$. This suggests that either the amplitudes of the leading corrections of $R^{(x)}$ and $R^{(a)}$ vanish identically, or at least that they are sufficiently small that they cannot be detected from our data. Due to these weak finite-size corrections, the values of p_c fitted from $R^{(x)}$ and $R^{(a)}$ are much more stable than those obtained from Q_1 and Q_2. From $R^{(x)}$ and $R^{(a)}$, we estimate $p_c = 0.248\,811\,82(10)$. For $R^{(3)}$, we report only the fits with corrections $b_1 L^{-1.2} + b_2 L^{-2}$. If y_i is left free the fits become unstable, regardless of whether the $b_2 L^{-2}$ term is included. From $R^{(3)}$, we estimate $p_c = 0.248\,811\,85(15)$ which is consistent with the value obtained from $R^{(x)}$ and $R^{(a)}$. From these fits, we estimate the universal wrapping probabilities to be $R_c^{(x)} = 0.257\,78(6)$, $R_c^{(a)} = 0.459\,97(8)$ and $R_c^{(3)} = 0.080\,41(8)$.

In Fig. 1, we illustrate our estimate of p_c by plotting $R^{(x)}$ and $R^{(a)}$ vs L. Precisely at $p = p_c$, as $L \to \infty$ the data should tend to a horizontal line, whereas the data with $p \neq p_c$ will bend upward or downward. Fig. 1 shows that our estimate of p_c lies slightly below the central value $0.248\,812\,6$ reported in [20].

In Fig. 2, we plot the data at $p = 0.248\,811\,8$ for $R^{(x)}$ and $R^{(a)}$ vs L^{-2}, and for Q_1 and Q_2 vs $L^{-1.2}$. The figure strongly suggests that the correction $L^{-1.2}$ dominates in Q_1 and Q_2, but vanishes (or is very weak) in $R^{(x)}$ and $R^{(a)}$.

B. Site percolation

For site percolation, we again estimate p_c by fitting Q_1, Q_2, and $R^{(x)}$, $R^{(a)}$, $R^{(3)}$ by Eq. (4). The fitting procedure is similar to that of bond percolation, and the results are summarized in Table II. From the table, we can see the fits of Q_1 and Q_2 are less stable for site percolation than bond percolation. The ratio χ^2/DF remains large until $L_{\min} \geq 32$ for Q_1 and $L_{\min} \geq 48$ for Q_2, and the resulting estimates of p_c range from $0.311\,606\,9(2)$ to $0.311\,607\,7(3)$.

The fits of the wrapping probabilities are better behaved, as was the case for bond percolation. For $R^{(3)}$, fixing $y_i = -1.2$ and including both the b_1 and b_2 terms, we find that b_1 is consistent with zero, while b_2 is clearly nonzero. Furthermore, if we set $b_2 = 0$ and leave y_i free, we find $y_i \approx -2$. This suggests that the amplitude of the leading correction of $R^{(3)}$ is smaller than the resolution of our fits, and might possibly be zero. The fits of the $R^{(a)}$ data, however, quite clearly indicate the presence of the $b_1 L^{-1.2}$ term. For $R^{(x)}$, we report only the fits with corrections $b_1 L^{-1.2} + b_2 L^{-2}$; if y_i is left free the fits become unstable, regardless of whether the $b_2 L^{-2}$ term is included. As for $R^{(a)}$, the amplitude b_1 appears to take a nonzero value. These observations suggest the leading correction $L^{-1.2}$ does not generically vanish for all wrapping probabilities, but rather that the amplitudes in some cases are smaller than the resolution of our simulations.

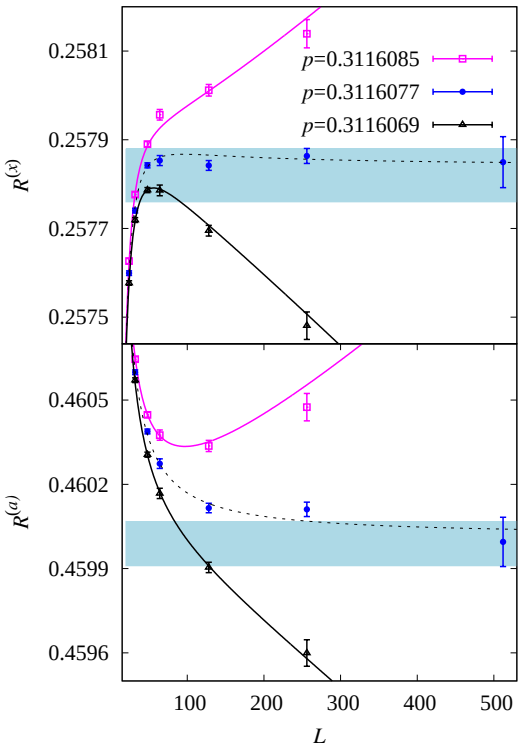

FIG. 3: Plots of $R^{(x)}(p, L)$ (top) and $R^{(a)}(p, L)$ (bottom) vs L for fixed values of p, for site percolation. In both cases, the curves correspond to our preferred fit of the MC data for $R(p, L)$ by ansatz (4); the dashed curve corresponds to setting $p = 0.311\,607\,7$. The blue strips indicate an interval of one sigma above and below the estimates $R_c^{(x)} = 0.257\,82(6)$ and $R_c^{(a)} = 0.459\,99(8)$.

Comparing the various fits, we estimate $p_c = 0.311\,607\,7(2)$ for site percolation, which is consistent with the previous result $0.311\,607\,7(4)$ [21]. In addition, we estimate the universal wrapping probabilities to be $R_c^{(x)} = 0.257\,82(6)$, $R_c^{(a)} = 0.459\,99(8)$, and $R_c^{(3)} = 0.080\,46(6)$, which are consistent with those estimated from bond percolation. In Fig. 3, we show plots of $R^{(x)}$ and $R^{(a)}$ which illustrate our estimate of p_c.

TABLE II: Fits of the wrapping probabilities $R^{(x)}, R^{(a)}, R^{(3)}$, and the ratios Q_1, Q_2 for site percolation. For $R^{(x)}$ we obtain unstable results when y_i is free.

	$L_{\min}$	χ^2/DF	p_c	y_t	$\mathcal{O}_c$	q_1	b_1	y_i	b_2
Q_1	32	19/16	0.311 606 9(2)	1.14(2)	0.865 05(2)	−0.22(2)	0.062(2)	−1.2	0(3)
	48	11/11	0.311 607 0(2)	1.11(3)	0.865 09(3)	−0.25(3)	0.054(6)	−1.2	0.2(2)
	64	3/6	0.311 607 7(3)	1.12(6)	0.865 26(7)	−0.24(6)	0.01(2)	−1.2	1.4(5)
	32	19/16	0.311 606 9(2)	1.15(2)	0.865 06(3)	−0.22(2)	0.063(4)	−1.11(2)	-
	48	10/11	0.311 607 1(2)	1.11(3)	0.865 12(4)	−0.25(3)	0.09(2)	−1.22(7)	-
	64	3/6	0.311 607 7(3)	1.12(6)	0.865 27(5)	−0.24(6)	0.9(10)	−1.8(3)	-
Q_2	64	3/6	0.311 607 6(2)	1.12(4)	0.633 3(1)	−0.56(9)	0.02(3)	−1.2	5.1(7)
	48	13/11	0.311 607 2(1)	1.14(2)	0.633 06(4)	−0.52(4)	0.9(1)	−1.52(3)	-
	64	2/6	0.311 607 6(2)	1.12(4)	0.633 29(8)	−0.56(9)	4(2)	−1.9(2)	-
$R^{(x)}$	16	42/39	0.311 607 85(5)	1.13(1)	0.257 89(2)	−0.76(4)	0.004(1)	−1.2	−0.22(1)
	24	30/31	0.311 607 74(6)	1.14(2)	0.257 84(3)	−0.75(5)	0.009(2)	−1.2	−0.29(3)
	32	24/24	0.311 607 66(7)	1.14(2)	0.257 80(3)	−0.73(5)	0.015(4)	−1.2	−0.39(6)
$R^{(a)}$	16	39/40	0.311 607 70(5)	1.12(2)	0.460 02(2)	−1.09(6)	0.023(2)	−1.2	0.08(2)
	24	25/32	0.311 607 67(7)	1.13(2)	0.459 99(4)	−1.05(6)	0.025(3)	−1.2	0.05(4)
	32	19/24	0.311 607 65(8)	1.13(2)	0.459 98(5)	−1.06(7)	0.027(6)	−1.2	0.02(9)
	16	36/40	0.311 607 75(6)	1.12(2)	0.460 06(3)	−1.09(6)	0.055(5)	−1.33(4)	-
	24	25/32	0.311 607 68(8)	1.13(2)	0.460 01(5)	−1.05(7)	0.039(9)	−1.21(9)	-
	32	19/24	0.311 607 65(9)	1.13(2)	0.459 99(7)	−1.06(7)	0.03(2)	−1.1(2)	-
$R^{(3)}$	16	50/38	0.311 608 01(8)	1.14(2)	0.080 55(1)	−0.38(3)	−0.010(8)	−1.2	−0.30(1)
	24	27/30	0.311 607 79(9)	1.14(2)	0.080 49(2)	−0.39(4)	−0.004(2)	−1.2	−0.38(3)
	32	18/23	0.311 607 65(11)	1.15(3)	0.080 45(3)	−0.38(4)	−0.002(3)	−1.2	−0.47(5)
	16	40/38	0.311 607 89(7)	1.15(2)	0.080 510(9)	−0.38(3)	−0.21(1)	−1.77(2)	-
	24	26/30	0.311 607 77(8)	1.14(2)	0.080 48(2)	−0.39(4)	−0.30(5)	−1.88(5)	-
	32	18/23	0.311 607 66(10)	1.15(3)	0.080 46(2)	−0.38(4)	−0.6(2)	−2.1(2)	-

IV. RESULTS AT p_c

In this section, we estimate the critical exponents y_t, y_h, and $d_{\min}$, as well as the excess cluster number. Fixing p at our estimated thresholds for bond and site percolation, we study the covariances $g_{bR}^{(x)}$ and $g_{sR}^{(x)}$, the mean size of the largest cluster C_1, the mean size of the cluster at the origin χ, the shortest-path length S, and the cluster density ρ. The MC data of $g_{bR}^{(x)}$, $g_{sR}^{(x)}$, C_1, χ and S are fitted by the ansatz

$$\mathcal{A} = L^{y_{\mathcal{A}}}(a_0 + b_1 L^{-1.2} + b_2 L^{-2}) \,. \tag{5}$$

We perform fits using different combinations of the two corrections $b_1 L^{-1.2}$ and $b_2 L^{-2}$ and compare the results.

A. Estimating y_t

We estimate y_t by studying the covariances $g_{bR}^{(x)}$ and $g_{sR}^{(x)}$, both of which scale as $\sim L^{y_t}$ at the critical point. We find this procedure for estimating y_t preferable to methods, such as that employed in [21], in which y_t is estimated by studying how quantities behave in the neighbourhood of p_c as the system deviates from criticality. In particular, we believe the current method produces more reliable error estimates.

We fit the data for $g_{bR}^{(x)}$ at $p = 0.248\,811\,8$ and $g_{sR}^{(x)}$ at $p = 0.311\,607\,7$ to Eq. (5), and the results are shown in Table III. The estimate of y_t from $g_{sR}^{(x)}$ produces a smaller error bar than that from $g_{bR}^{(x)}$. From these fits we take our final, somewhat conservative, estimate to be $y_t = 1.141\,0(15)$.

TABLE III: Fits of covariances $g_{bR}^{(x)}$ and $g_{sR}^{(x)}$.

	$L_{\min}$	χ^2/DF	y_t	a_0	b_1	b_2
$g_{bR}^{(x)}$	16	4/4	1.140 4(9)	0.231(1)	−0.03(2)	0.1(2)
	24	4/3	1.140 6(13)	0.231(2)	−0.02(5)	0.0(4)
	16	4/5	1.140 9(4)	0.230 7(3)	−0.012(3)	-
	24	4/4	1.140 6(6)	0.231 1(6)	−0.017(7)	-
$g_{sR}^{(x)}$	16	5/4	1.141 6(4)	0.155 1(3)	−0.004(7)	−0.06(5)
	24	4/3	1.141 1(6)	0.155 4(6)	−0.02(2)	−0.1(2)
	16	7/5	1.141 1(2)	0.155 5(1)	−0.013(1)	-
	24	4/4	1.141 4(3)	0.155 3(2)	−0.010(2)	-

In Fig. 4, we plot $(\ln g_{bR}^{(x)} - y_t \ln L)$ and $(\ln g_{sR}^{(x)} - y_t \ln L)$ vs $\ln L$ using three different values of y_t: our estimate, as well as our estimate plus or minus three standard deviations. Using the true value of y_t should produce a horizontal line for large L. In the figure, the data using $y_t = 1.136\,5$ and $y_t = 1.145\,5$ respectively bend upward and downward, suggesting that the true value of y_t does indeed lie within 3 sigmas of our estimate. The data with $y_t = 1.141$ appear to be consistent with an asymptotically horizontal line. We note that while the curve appears to be increasing around the point at $L = 512$ for bond percolation, it instead slightly decreases for site per-

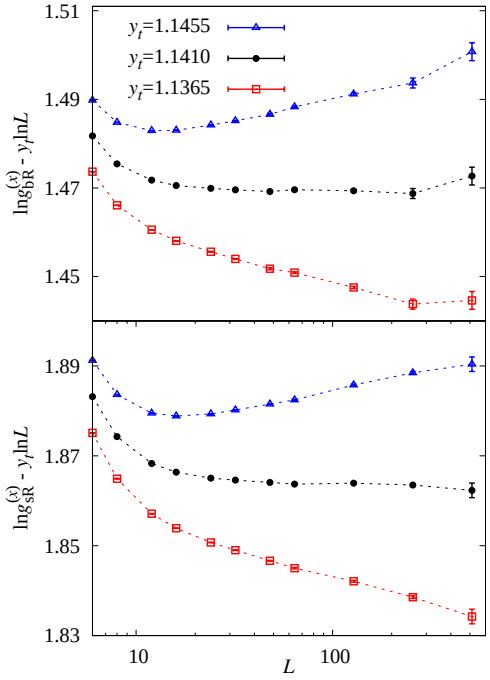

FIG. 4: Plots of $(\ln g_{bR}^{(x)} - y_t \ln L)$ (top) and $(\ln g_{sR}^{(x)} - y_t \ln L)$ (bottom) vs $\ln L$ illustrating our estimate $y_t = 1.141\,0(15)$. The dashed curves are simply to guide the eye.

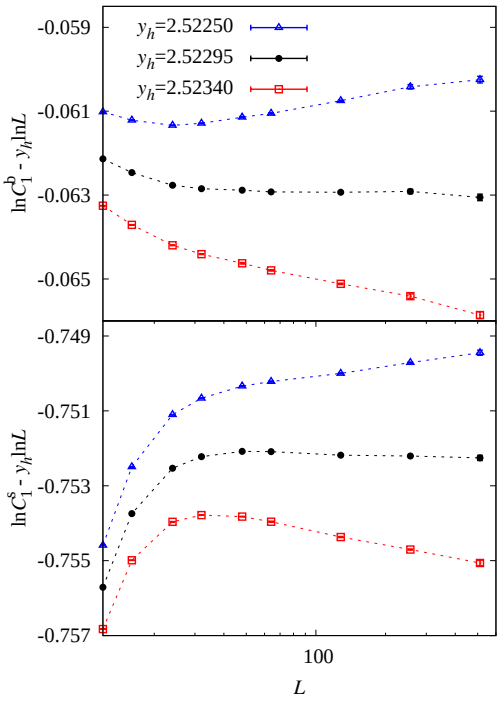

FIG. 5: Plots of $(\ln C_1^b - y_h \ln L)$ (top) and $(\ln C_1^s - y_h \ln L)$ (bottom) vs $\ln L$ to show our estimate $y_h = 2.522\,95(15)$. The dashed curves are simply to guide the eye.

TABLE IV: Fits of C_1 and χ. The superscripts b and s denote bond and site percolation, respectively.

	$L_{\min}$	χ^2/DF	y_h	a_0	b_1	b_2
C_1^b	16	3/4	2.522 86(5)	0.939 4(3)	−0.014(6)	0.22(4)
	24	3/3	2.522 89(7)	0.939 3(4)	−0.009(11)	0.2(1)
	24	5/4	2.522 98(3)	0.938 8(2)	0.009(2)	-
	32	3/3	2.522 94(4)	0.939 0(2)	0.005(3)	-
χ^b	16	4/4	2.523 03(4)	1.125 7(5)	0.14(1)	0.18(7)
	24	3/3	2.523 00(5)	1.126 2(7)	0.12(2)	0.3(2)
	24	6/4	2.523 08(3)	1.125 1(3)	0.157(4)	-
	32	4/3	2.523 05(3)	1.125 5(4)	0.151(6)	-
C_1^s	16	5/4	2.522 99(3)	0.471 16(7)	0.024(2)	−0.44(2)
	24	5/3	2.523 00(5)	0.471 1(2)	0.024(4)	−0.45(4)
χ^s	32	0.9/2	2.522 91(5)	0.284 1(2)	−0.001(7)	−1.15(9)
	48	0.7/1	2.522 94(9)	0.284 0(4)	−0.007(18)	−1.3(3)
	32	0.9/3	2.522 92(1)	0.284 06(3)	-	−1.16(1)
	48	0.9/2	2.522 91(2)	0.284 08(7)	-	−1.17(5)

colation, suggesting that in fact this movement is dominated (or even entirely caused) by noise.

B. Estimating y_h

We estimate y_h by studying the divergence of C_1 and χ as L increases with p fixed to our best estimates of p_c. We fit the MC data for C_1 and χ by Eq. (5), with the exponent $y_{\mathcal{A}}$ then corresponding to y_h and $2y_h - d$, respectively. The results are reported in Table IV. We use superscripts b and s to distinguish bond and site percolation. For C_1^b and χ^s, the amplitude b_1 is quite small, while b_1 in χ^b and C_1^s is clearly present. In the fits of χ^s with one correction term $b_1 L^{-1.2}$, the ratio χ^2/DF remains large until $L_{\min} \geq 64$. We therefore show the fits with correction $b_2 L^{-2}$ instead. Comparing these fits, we estimate $y_h = 2.522\,95(15)$.

TABLE V: Fits of S. The superscripts b and s denote bond and site percolation, respectively.

	$L_{\min}$	χ^2/DF	$d_{\min}$	a_0	b_1	b_2
S^b	24	2/3	1.375 26(5)	1.814 9(5)	−0.65(2)	−3.8(2)
	32	1/2	1.375 33(7)	1.814 2(7)	−0.59(5)	−4.4(4)
	48	0/2	1.375 30(9)	1.815(1)	−0.63(9)	−4(1)
S^s	16	5/4	1.375 80(2)	1.383 4(2)	−3.432(5)	2.72(3)
	24	4/4	1.375 77(3)	1.383 6(3)	−3.45(2)	2.82(3)
	32	4/2	1.375 76(5)	1.383 7(4)	−3.45(3)	2.9(3)

In Fig. 5, we plot $(\ln C_1^b - y_h \ln L)$ and $(\ln C_1^s - y_h \ln L)$ vs $\ln L$ using three different values of y_h: our estimate, as well as our estimate plus or minus three standard deviations. As L increases, the data with $y_h = 2.522\,50$ and $2.523\,40$ respectively slope upward and downward, while the data with $y_h = 2.522\,95$ are consistent with an asymptotically horizontal line.

TABLE VI: Fits of ρ. The superscripts b and s denote bond and site percolation, respectively.

	$L_{\min}$	χ^2/DF	ρ_c	b	b_1
ρ^b	16	3/5	0.272 932 83(1)	0.679(3)	0.1(6)
	24	1/4	0.272 932 83(1)	0.674(6)	3(4)
	16	2/7	0.272 932 83(1)	0.678 9(6)	-
	24	2/6	0.272 932 83(1)	0.679(2)	-
ρ^s	12	4/6	0.052 438 218(3)	0.674 5(5)	0.02(8)
	16	4/5	0.052 438 218(3)	0.674 7(8)	−0.02(21)
	24	4/4	0.052 438 218(3)	0.674(2)	0.2(10)
	12	4/7	0.052 438 218(3)	0.674 6(2)	-
	16	4/6	0.052 438 218(3)	0.674 6(3)	-
	24	4/5	0.052 438 218(3)	0.674 6(5)	-

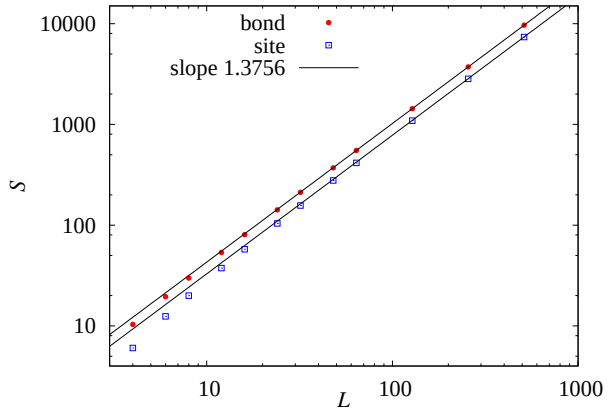

FIG. 6: Log-log plot of S versus L for bond and site percolation. Two straight lines with slope 1.375 6 are included for comparison.

C. Estimating $d_{\min}$

We estimate the shortest-path fractal dimension $d_{\min}$ by studying the quantity S at our estimated thresholds. The MC data for S are fitted to Eq. (5) with the exponent $y_{\mathcal{A}}$ replaced by $d_{\min}$, and the results are reported in Table V. We again use the superscripts b and s to distinguish bond and site percolation. In the fits, both b_1 and b_2 are clearly observable for S^b and S^s. And when we set $b_2 = 0$, the ratio χ^2/DF remains relatively large. We also did the fits by replacing the correction with b_2 by a constant term c_0 in Eq. (5), and obtained $d_{\min}$(bond) = 1.375 55(6) and $d_{\min}$(site) = 1.375 59(6). Comparing these fits, we estimate $d_{\min} = 1.375\,6(3)$.

To illustrate this estimate, Fig. 6 shows a log-log plot of S versus L.

D. Excess number of clusters

The cluster density tends to a finite limit $\rho_c = \lim_{L\to\infty}\lim_{p\to p_c}\rho$ at criticality. While the value of ρ_c is non-universal, the *excess cluster number* $b := \lim_{L\to\infty}\lim_{p\to p_c} L^d(\rho - \rho_c)$ is universal [27]. To estimate b, we study ρ with p fixed to our estimated thresholds for bond and site percolation and fit the data to the ansatz

$$\rho = \rho_c + L^{-3}(b + b_1 L^{-2}) \; . \tag{6}$$

The resulting fits are summarized in Table VI, where we again use superscripts b and s to differentiate the bond and site cases. We report fits both with b_1 free and $b_1 = 0$. We find that ρ can be well fitted to (6) with $b_1 = 0$ fixed. Leaving b_1 free, we find that b_1 is consistent with zero, suggesting that the leading correction exponent might be even smaller than -2. We also performed fits in which the leading correction exponent was fixed to -1.2 and -3, and in both cases the resulting estimates of ρ_c and b were consistent with those reported in Table VI. Leaving the leading correction exponent free produces unstable fits however. Comparing these fits, we estimate $b = 0.675(2)$.

To our knowledge, no estimates of b on the periodic $L \times L \times L$ simple cubic lattice have previously been reported in the literature; on the $L \times L$ square lattice $b = 0.883\,5(8)$ [27]. The excess cluster number was studied in [20] on an $L \times L \times L'$ lattice with $L' \gg L$. Naively, extrapolating their results to $L' = L$ gives an estimate of $b \approx 0.412$ which is significantly below our estimate. We also note that our estimate of the number of clusters $\rho_c = 0.272\,932\,83(1)$ differs slightly with the estimate $\rho_c = 0.272\,931\,0(5)$ reported in [20].

V. DISCUSSION

We study in this paper standard bond and site percolation on the three-dimensional simple-cubic lattice with periodic boundary conditions. Using extensive Monte Carlo simulations and finite-size scaling analysis, we report the estimates: $p_c = 0.248\,811\,82(10)$ (bond) and $p_c = 0.311\,607\,7(2)$ (site). The bulk thermal and magnetic exponents are estimated to be $y_t = 1.141\,0(15)$ and $y_h = 2.522\,95(15)$, the shortest-path fractal dimension to be $d_{\min} = 1.375\,6(3)$, and the leading irrelevant exponent to be $y_i = -1.2(2)$. The universal value of the excess cluster number is estimated to be $b = 0.675(2)$.

We emphasize that the reported estimates of p_c are obtained by studying wrapping probabilities, which are found to have weaker corrections to scaling than dimensionless ratios constructed from moments of magnetic quantities such as $\mathcal{C}_1$ and $\mathcal{S}_m$. In particular, we find evidence suggesting the leading correction exponent in certain wrapping probabilities ($R^{(x)}$ and $R^{(a)}$ for bond percolation, $R^{(3)}$ for site percolation) may be ≈ -2 rather than -1.2, although the reasons are not clear. The universal values of the wrapping probabilities we studied are estimated to be: $R_c^{(x)} = 0.257\,80(6)$, $R_c^{(a)} = 0.459\,98(8)$, and $R_c^{(3)} = 0.080\,44(8)$, by comparing the results for bond and site percolation.

TABLE VII: Summary of estimated thresholds, critical exponents, universal wrapping probabilities, and excess cluster number of bond and site percolation on the simple-cubic lattice. We note that the values of y_t and y_h in [21] marked by superscript $*$ contained typographical errors. The final error bars reported in [21] were also underestimated, taking insufficient account of systematic errors.

Ref.	p_c(bond)	p_c(site)	$y_t = 1/\nu$	$y_h = d_f$	$d_{\min}$	y_i	$R^{(x)}$	$R^{(a)}$	$R^{(3)}$	b
[20]	0.248 812 6(5)		1.12(2)	2.523(4)						
[22]		0.311 608 0(4)								
[23]		0.311 608 1(13)	1.141(2)	2.523 0(3)		−1.61(13)				
[17]	0.249 0(2)	0.311 5(3)	1.15(2)				0.265(6)	0.471(8)	0.084(4)	
[21]		0.311 607 7(4)	1.145 0(7)*	2.522 6(1)*						
[24]	0.248 812 0(5)		1.142(3)	2.523 5(8)						
[25]					1.375 6(6)					
[26]			1.142(8)			−1.0(2)				
This work	0.248 811 82(10)	0.311 607 7(2)	1.141 0(15)	2.522 95(15)	1.375 6(3)	−1.2(2)	0.257 80(6)	0.459 98(8)	0.080 44(8)	0.675(2)

From these values we can estimate other wrapping probabilities discussed in the literature, such as

$$\begin{aligned} R^{(1)} &:= \langle \mathcal{R}^{(x)}(1-\mathcal{R}^{(y)})(1-\mathcal{R}^{(z)})\rangle \\ &= \frac{1}{3}(2R^{(a)} + R^{(3)} - 3R^{(x)}) \,, \\ R^{(2)} &:= \langle \mathcal{R}^{(x)}\mathcal{R}^{(y)}(1-\mathcal{R}^{(z)})\rangle \\ &= \frac{1}{3}(3R^{(x)} - 2R^{(3)} - R^{(a)}) \,, \\ R^{(x,y)} &:= \langle \mathcal{R}^{(x)}\mathcal{R}^{(y)}\rangle = \frac{1}{3}(3R^{(x)} + R^{(3)} - R^{(a)}) \,. \end{aligned}$$

In words, $R^{(1)}$ is the probability that a winding exists in one given direction but not in the other two directions; $R^{(2)}$ is the probability that a winding exists in two given directions but not in the third; and $R^{(x,y)}$ is the probability that a winding exists in two given directions, regardless of whether a winding exists in the third direction. We obtain $R_c^{(1)} = 0.075\,67(14)$, $R_c^{(2)} = 0.050\,85(14)$, and $R_c^{(x,y)} = 0.131\,29(12)$.

Table VII summarizes the estimates presented in this work. For comparison, we also provide an (incomplete) summary of previous estimates.

VI. ACKNOWLEDGMENTS

This research was supported in part by NSFC under Grant No. 91024026 and 11275185, and the Chinese Academy of Science. It was also supported under the Australian Research Council's (ARC) Discovery Projects funding scheme (project number DP110101141), and T.G. is the recipient of an Australian Research Council Future Fellowship (project number FT100100494). YD is grateful for the hospitality of Monash University at which this work was partly completed. The simulations were carried out on the NYU-ITS cluster, which is partly supported by NSF Grant No. PHY-0424082.

[1] S. R. Broadbent and J. M. Hammersley, Proceedings of the Cambridge Philosophical Society **53**, 629 (1957).
[2] D. Stauffer and A. Aharony, *Introduction To Percolation Theory* (Taylor & Francis, London, 1994), 2nd ed.
[3] G. R. Grimmett, *Percolation* (Springer, Berlin, 1999), 2nd ed.
[4] B. Bollobás and O. Riordan, *Percolation* (Cambridge University Press, 2006).
[5] B. Nienhuis, in *Phase Transition and Critical Phenomena*, edited by C. Domb, M. Green, and J. L. Lebowitz (Academic Press, London, 1987), vol. 11.
[6] J. L. Cardy, in *Phase Transition and Critical Phenomena*, edited by C. Domb, M. Green, and J. L. Lebowitz (Academic Press, London, 1987), vol. 11.
[7] S. Smirnov and W. Werner, Math. Res. Lett. **8**, 729 (2001).
[8] J. W. Essam, in *Phase Transition and Critical Phenomena*, edited by C. Domb and M. S. Green (Academic Press, New York, 1972), vol. 2.
[9] H. Kesten, Commun. Math. Phys. **74**, 41 (1980).
[10] G. Toulouse, Nuovo Cimento Soc. Ital. Fis. **B 23**, 234 (1974).
[11] M. Aizenman and C. M. Newman, J. Stat. Phys. **36**, 107 (1984).
[12] T. Hara and G. Slade, Commun. Math. Phys. **128**, 333 (1990).
[13] R. P. Langlands, C. Pichet, P. Pouliot, and Y. Saint-Aubin, J. Stat. Phys. **67**, 553 (1992).
[14] J. Cardy, J. Phys. A **25**, L201 (1992).
[15] R. Langlands, P. Pouliot, and Y. Saint-Aubin, Bull. Am. Math. Soc. **30**, 1 (1994).
[16] H. T. Pinson, J. Stat. Phys. **75**, 1167 (1994).
[17] P. H. L. Martins and J. A. Plascak, Phys. Rev. E **67**, 046119 (2003).
[18] M. E. J. Newman and R. M. Ziff, Phys. Rev. Lett. **85**, 4104 (2000).
[19] X. Feng, Y. Deng, and H. W. J. Blöte, Phys. Rev. E **78**, 031136 (2008).
[20] C. D. Lorenz and R. M. Ziff, Phys. Rev. E **57**, 230 (1998).
[21] Y. Deng and H. W. J. Blöte, Phys. Rev. E **72**, 016126 (2005).
[22] C. D. Lorenz and R. M. Ziff, J. Phys. A **31**, 8147 (1998).

[23] H. G. Ballesteros, L. A. Fernández, V. Martín-Mayor, A. Muñoz Sudupe, G. Parisi, and J. J. Ruiz-Lorenzo, J. Phys. A **32**, 1 (1999).
[24] Z. Zhou, J. Yang, R. M. Ziff, and Y. Deng, Phys. Rev. E **86**, 021102 (2012).
[25] Z. Zhou, J. Yang, Y. Deng, and R. M. Ziff, Phys. Rev. E **86**, 061101 (2012).
[26] B. Kozlov and M. Laguës, Physica A **389**, 5339 (2010).
[27] R. M. Ziff, S. R. Finch, and V. S. Adamchik, Phys. Rev. Lett. **79**, 3447 (1997).
[28] The tar file unpacks to make a directory `percolation` with subdirectories `bond` and `site`. Individual files have names like `C1_bond.txt` or `CHI_site.txt` and have four fields on each line: L, p, value and error bar.